NOAA Technical Report NESDIS 84

SPURIOUS SEMI-DIURNAL VARIATION IN THE E.R.B.E. OUTGOING LONGWAVE RADIATION

Washington, D.C.
June 1995

U.S. DEPARTMENT OF COMMERCE
National Oceanic and Atmospheric Administration
National Environmental Satellite, Data, and Information Service

NOAA TECHNICAL REPORTS

National Environmental Satellite, Data, and Information Service

ironmental Satellite, Data, and Information Service (NESDIS) manages the Nation's civil Earth-stems, as well as global national data bases for meteorology, oceanography, geophysics, and solar-rom these sources, it develops and disseminates environmental data and information products on of life and property, national defence, the national economy, energy development and distri-upplies, and the development of natural resources.

Publication in the NOAA Technical Report series does not preclude later publication in scientific journals in expanded or modified form. The NESDIS series of NOAA Technical Reports is a continuation of the former NESS and EDIS series of NOAA Technical Reports and the NESC and EDS series of Environmental Science Services Administration (ESSA) Technical Reports.

A limited number of copies are available by contacting Nancy Everson, NOAA/NESDIS, E/RA22, 5200 Auth Road, Washington D.C., 20233. Copies can also be ordered from the National Technical Information Service (NTIS), U.S. Department of Commerce, Sills Bldg., 5285 Port Royal Road, Springfield, VA. 22161, (703) 487-4650 (prices on request for paper copies or microfiche, please refer to PB number when ordering). A partial listing of more recent reports appear below:

NESDIS 26 Monthly and Seasonal Mean Outgoing Longwave Radiation and Anomalies. Arnold Gruber, Marylin Varnadore, Phillip A. Arkin and Jay S. Winston, October 1987. (PB87 160545/AS)

NESDIS 27 Estimation of Broadband Planetary Albedo from Opertional Narrowband Satellite Measurements. James Wydick, April 1987. (PB88 107644/AS)

NESDIS 28 The AVHRR/HIRS Operational Method for Satellite Based Sea Surface Temperature Determination. Charles Walton, March 1987. (PB88 107594/AS)

NESDIS 29 The Complementary Roles of Microwave and Infrared Instruments in Atmospheric Soundings. Larry McMillin, February 1987. (PB87 184917/AS)

NESDIS 30 Planning for Future Operational Sensors and Other Priorities. James C. Fischer, June 1987. (PB87 220802/AS)

NESDIS 31 Data Processing Alogorithms for Inferring Stratospheric Gas Concentrations from Balloon-Based Solar Occultation Data. I-Lok Chang (American University) and Michael P. Weinreb, April 1987. (PB87 196424)

NESDIS 32 Precipitation Detection with Satellite Microwave Data. Yang Chenggang and Andrew Timchalk, June 1988. (PB88 240239)

NESDIS 33 An Introduction to the GOES I-M Imager and Sounder Instruments and the GVAR Retransmission Format. Raymond J. Komajda (Mitre Corp) and Keith McKenzie, October 1987. (PB88 132709)

NESDIS 34 Balloon-Based Infrared Solar Occultation Measurements of Stratospheric 03, H20, HNo3, and CF2C12. Michael P. Weinreb and I-Lok Chang (American University), September 1987. (PB88 132725)

NESDIS 35 Passive Microwave Observing From Environmental Satellites, A Status Report Based on NOAA's June 1-4, 1987, Conference in Williamsburg, VA. James C. Fisher, November 1987. (PB88 208236)

NESDIS 36 Pre-Launch Calibration of Channels 1 and 2 of the Advanced Very High Resolution Radiometer. C. R. Nagaraja Rao, October 1987. (PB88 157169/AS)

NESDIS 39 General Determination of Earth Surface Type and Cloud Amount Using Multispectral AVHRR Data. Irwin Ruff and Arnold Gruber, February 1988. (PB88 199195/AS)

NESDIS 40 The GOES I-M System Functional Description. Carolyn Bradley (Mitre Corp), November 1988.

NESDIS 41 Report of the Earth Radiation Budget Requirements Review - 1987, Rosslyn, VA, 30 March-3 April 1987. Larry L. Stowe (Editor), June 1988.

NESDIS 42 Simulation Studies of Improved Sounding Systems. H. Yates, D. Wark, H. Aumann, N. Evans, N. Phillips, J. Sussking, L. McMillin, A. Goldman, M. Chahine and L. Crone, February 1989.

NESDIS 43 Adjustment of Microwave Spectral Radiances of the Earth to a Fixed Angle of Progagation. D. Q. Wark, December 1988. (PB89 162556/AS)

NESDIS 44 Educator's Guide for Building and Operating Environmental Satellite Receiving Stations. R. Joe Summers, Chambersburg Senior High, February 1989.

NESDIS 45 Final Report on the Modulation and EMC Consideration for the HRPT Transmission System in the Post NOAA-M Polar Orbiting Satellite ERA. James C. Fisher (Editor), June 1989. (PB89 223812/AS)

NESDIS 46 MECCA Program Documentation. Kurt W. Hess, September 1989.

NESDIS 47 A General Method of Using Prior Information in a Simultaneous Equation System. Lawrence J. Crone, David S Crosby and Larry M. McMillin, October 1989.

NOAA Technical Report NESDIS 84

SPURIOUS SEMI-DIURNAL VARIATION IN THE E.R.B.E. OUTGOING LONGWAVE RADIATION

Chandrasekhara R. Kondragunta
Cooperative Institute for Climate Studies
Department of Meteorology
University of Maryland
College Park, MD 20742

and

Arnold Gruber
Office of Research and Applications

Washington, D.C.
June 1995

U.S. DEPARTMENT OF COMMERCE
Ronald H. Brown, Secretary

National Oceanic and Atmospheric Administration
D. James Baker, Under Secretary

National Environmental Satellite, Data, and Information Service
Robert S. Winokur, Assistant Administrator

Spruious Semi-diurnal Variation in the E.R.B.E. Outgoing Longwave Radiation

Table of Contents

		Page
Abstract		2
1.	Introduction	3
2.	Data and Analysis Procedure	4
3.	Results	6
4.	Discussion	7
5.	Concluding Remarks	10
Acknowledgements		11
References		12
List of Tables		13
List of Figures		14

Abstract

The Outgoing Longwave Radiation (OLR) data from the Earth Radiation Budget Experiment (ERBE) were analyzed for the period during which all three ERBE satellites were operating i.e. December 6, 1986 to January 19, 1987, to study the diurnal variation. A cubic spline interpolation technique was used to fill the gaps between the sampled hours of OLR. The interpolated data was composited to obtain mean diurnal time series of OLR. In order to extract the diurnally varying dominant modes, an Empirical Orthogonal Function (EOF) analysis technique was applied to the normalized anomalies of the composite daily OLR.

The first EOF mode explains 53.2% of the total normalized variance. Its spatial pattern is dominated by positive loadings located over the oceanic cloudy regions and its temporal variation indicate a strong semi-diurnal cycle with maxima and minima coinciding with the equator crossing times of the NOAA-9 and NOAA-10 satellites. It is argued that the semi-diurnal cycle noticed in this mode is not realistic and is caused by biases in retrieving OLR from different instruments on board NOAA-9 and NOAA-10 . The temporal variation of the second EOF mode indicate a true diurnal signal with most of the spatial variation occurring over the dry continental regions. In the third EOF mode, most of the variation is over cloudy regions, whose temporal variation indicate a semi-diurnal variation modulated by a large amplitude diurnal cycle. The effect of this instrumental bias is clearly evident in the global averages of the OLR.

1. Introduction

The earth's climate system varies on various spatial and temporal scales. To fully understand the climate, knowledge of its spatial and temporal variation is crucial. Top of the atmosphere radiation budget parameters have proven to be good indicators of climate variations on annual and interannual time scales. Though these radiation budget parameters can be measured instantaneously with acceptable accuracy with current remote sensing techniques, their temporal sampling is inadequate especially on a diurnal time scale to obtain reasonable daily and monthly means. To rectify this diurnal sampling problem, the National Aeronautics and Space Administration (NASA) launched an experiment called the Earth Radiation Budget experiment (ERBE) (Barkstrom, B. R., 1984). The ERBE is comprised of three satellites, one in a mid inclined (57°) precessing orbit and two in polar orbits with different equator crossing times. This orbital configuration was aimed at achieving diurnal sampling adequate enough to obtain reasonable diurnally averaged radiation budget parameters (Brooks and Minnis, 1984).

Each of these satellites carried scanning and non-scanning radiometers. The scanning instruments measured radiances in three spectral intervals viz. shortwave (.2-5μm), longwave (5-50μm) and total (.2-50μm). The non- scanning instruments are still operating and they measure radiances in two spectral intervals viz. shortwave (.2-5 μm) and total (.2-50 μm). The Outgoing Longwave Radiation (OLR) from the scanner is obtained as a difference between the total and shortwave channel fluxes during daytime and the flux from the total channel during nighttime. Initially only two satellites were launched, one in polar orbit (NOAA-9: equator crossing time 2:30 P.M. local time) and the other in precessing orbit (Earth Radiation Budget Satellite, ERBS). It was not until November of 1986, when the third satellite (NOAA-10: equator crossing time 7:30 A.M. local time) was launched in a polar orbit. Unfortunately, the scanning instrument on the NOAA-9 ceased operating on January 19, 1987. As a result, there was only a period of 45 days, between December 6, 1986, and January 19, 1987, during which the scanner instruments on all three satellites were operating continuously. In this study, the OLR data obtained during this 45 day period were analyzed to study the diurnal variation.

Depending on the cloud and geographic scene types, the ERBE data processing scheme uses a combination of a linear and half sine diurnal model to fill in the missing longwave values (Brooks et al, 1986). The half-sine diurnal model with phase angle fixed at local noon is used for clear-sky conditions over land and desert geographic types. The criteria to apply this half-sine model are (i) there must be at least one daytime measurement located more than 1 hour from the terminator, (ii) there must be at least one nighttime measurement, (iii) the least square sine wave fit to the daytime data must have a positive amplitude, (iv) the peak value of the daytime fit must not exceed 400 Wm^{-2} and (v) the length of the day must exceed 2 hours. The linear interpolation technique is applied at all times and for all scene types. Though this diurnal scheme gives reasonable estimates of the monthly mean OLR, it does not necessarily represent the true climatological diurnal variation of the broadband OLR especially

over deserts and clear-sky land regions, because of its heavy dependence on the half sine model. Cheruy et al. (1991) analyzed NOAA-9 and ERBS combined data set for the months of April and July 1985 over tropical Africa and neighboring Atlantic regions and compared it with METEOSAT observations. They concluded that a combination of two Sun synchronous polar orbiting satellites and one mid inclined precessing satellite would eliminate most of the diurnal sampling errors. Motivated by their conclusion, we made an attempt to analyze the OLR data from the 45 day period during which all three ERBE scanners operated simultaneously.

2. Data and Analysis Procedure

The ERBE data analyzed in this study are top of the atmosphere radiation fluxes available on the ERBE S-9 data tape. It consists of monthly mean products, daily products which are based on observed and model built values, and actual sampled hourly values, on a 2.5° longitude x latitude resolution. A description of the archived ERBE data product, ERBE instruments and data processing is given by Barkstrom et al. (1989). Actual sampled hourly fluxes of OLR for average sky conditions were extracted from the S-9 data tape for the three satellite combination period, December 6, 1986 to January 19, 1987. First, sampling of OLR was examined to get an idea of the feasibility of performing a diurnal variation study. Sampling of the OLR from the three satellites was examined for every grid point in the latitudinal direction and every fifth grid point in the longitudinal direction. Table 1 shows the average sky OLR sampling of each local hour for every other latitude band centered at 1.25°E. The number in each column indicates the number of times that particular local hour was sampled by all three satellites together. As one can see from this table, sampling is good covering many local hours at higher latitudes where there is an overlap in the coverage by scanners on board polar orbiting satellites. As expected, high frequency of sampling is noticed at local hours approximately 1530 LST (0330 LST); and 1930 LST (0730 LST) during the ascending (descending) nodes of the NOAA-9 and the NOAA-10, respectively. The hours not sampled well by the polar orbiting satellites are filled by the ERBS. Since ERBS samples only up to 57° latitude in either hemisphere, one can notice gaps in sampling poleward of that latitude. The sampling pattern by polar orbiters is similar to this at other longitudes as well, except the local hours sampled by the ERBS change.

As a preliminary analysis, a composite diurnal variation of OLR was obtained by averaging all sampled observations at each local hour over the entire study period at a few selected grid points. This showed a sampling bias to the heavily sampled local hours by the NOAA-9 and NOAA-10 satellites. The local hours that were not sampled by either of these two satellites were sampled only once or twice during the entire study period by the ERBS. Some local hours were not sampled at all. Furthermore, due to the precessing nature of the ERBS, whatever values sampled by it are representative of the synoptic conditions present at the time of sampling rather than the average conditions of the entire study period. Therefore, the composite diurnal variation obtained by this procedure did not appear to be realistic.

Hence this analysis procedure was discarded and a different procedure was followed as described below.

All the sampled hourly OLR observations starting from December 6, 1986, to January 19, 1987, were arranged sequentially. A cubic spline interpolation technique was used to fill the data gaps. Cubic spline interpolation technique takes the slope of the observations into account when interpolating. A segment of the time series obtained from both the linear interpolation between the observations and the cubic spline technique are shown in figure 1, for a region over the Sahara where the diurnal variation of OLR clearly follows the diurnal variation of surface temperature. The time series obtained from cubic spline interpolation is smoother than the one obtained from the simple linear interpolation. A composite diurnal cycle using interpolated (cubic spline) data was obtained by grouping the observations by local hour and averaging them over all 45 days. The composite diurnal variation for the grid point over the Sahara is shown in figure 2. For comparison purposes, monthly mean (average of December '86 and January '87) OLR diurnal cycle extracted from the ERBE S-9 tape is also produced in figure 2. This diurnal cycle was constructed by the ERBE data processing algorithm (Brooks et al, 1986) and depends on the linear interpolation and half sine model when certain criteria, explained earlier, are met. The diurnal variation obtained from cubic spline (solid curve) shows a maximum in OLR at 1400 LST and a minimum around 0400 to 0500 LST. To a first approximation, this OLR diurnal behavior follows the diurnal surface temperature behavior over the deserts with peak occurring in the afternoon and slowly cooling off until after sunrise the following morning (Rosenberg et al.,1983; Riehl, 1979; and Harrison et al. 1988). The diurnal variation from the monthly means (dotted curve) show a peak at 1300 LST. This is biased to the half-sine diurnal model in the analysis, which uses a peak at local noon. It is evident from these curves that with the satellite configuration used in the ERBE, one can obtain a realistic diurnal cycle of the OLR without resorting to any diurnal modeling. The small differences in diurnal amplitude may be attributed to the differences in the analysis procedures.

In order to give equal importance to all grid points in the analysis, the composite daily mean was subtracted and the anomalies were normalized by the standard deviation at each grid point. An Empirical Orthogonal Function (EOF) analysis technique was applied to the normalized OLR anomalies to obtain diurnally varying dominant spatial modes. Unlike harmonic analysis whose temporal variation is constrained by sinusoidal diurnal, semi-diurnal etc. variations, the time variation of EOF modes are selected such that they represent the diurnal variation of the dominant modes with maximum explained normalized variance. This technique was applied widely in climate research to study the temporal and spatial variation of various parameters (for example, Kutzbach, 1967, Kidson, 1975, Smith et al, 1990, Kondragunta and Gruber, 1994) and also to obtain the systematic instrumental biases, especially in satellite data (Chelliah and Arkin, 1992).

3. Results

In order to give meaningful interpretation, the spatial patterns of the EOF modes are expressed in terms of correlation coefficients. These are the correlations between normalized anomaly time series and the respective eigen function at each grid point. A positive (negative) correlation coefficient in the spatial map indicates that the actual normalized anomaly time series is positively (negatively) correlated with the time variation of that eigen mode. For example, at a grid point where the correlation coefficient is positive in the spatial pattern (Fig. 3a), the diurnal variation of OLR is such that it has positive peaks at 0800 LST and 2000 LST (Fig. 3b). Similarly, at a grid point where the correlation coefficient is negative (Fig. 3a), the diurnal variation of OLR is such that it has positive peaks at 0400 LST and 1500 LST. These correlations can also give the local variance explained by that particular eigen mode at each grid point by simply taking the square of the correlation coefficient.

Presented in figs. 3a and 3b are the spatial patterns of the EOF-1 and its time variation, respectively. Most of the spatial loadings are positive and they occur mostly over the oceanic regions. The time variation of this pattern indicate a semi-diurnal variation, with maxima at 0800 LST and 2000 LST and minima at 0400 LST and 1500 LST. It is important to note that these maxima and minima coincide with the equator crossing times of the NOAA-10 and NOAA-9, respectively. The systematically positive correlations heavily weighted to the southern hemisphere, in this case, indicate some kind of bias in the data. Moreover, these high positive correlations occur mostly over the oceanic cloudy regions which indicate that the bias is related somehow to retrieval of OLR from cloudy scenes. At this point it is our conjecture that the semi-diurnal cycle shown in this mode is not the true diurnal variation of OLR and is caused by biases in retrieving OLR from different instruments. This point is discussed more extensively in the next section. There is also an indication that the semi-diurnal variation in this mode is modulated by a diurnal cycle. However, the phase of this diurnal cycle are not in agreement with the earlier studies (Gruber and Chen, 1989, Hartman and Recker, 1986, Kondragunta et al, 1993, Minnis and Harrison, 1984 and Meisner and Arkin, 1987). This disagreement again confirms that the diurnal variation shown in this mode is not realistic. This mode explains 53.2% of the normalized variance.

Presented in fig 4a and 4b are the spatial pattern of the EOF-2 and the associated time variation, respectively. The spatial pattern clearly shows high positive correlations over the dry continental regions. The time variation indicate a strong diurnal signal. This mode indicates that over the continental regions, OLR is maximum at 1500 LST and minimum at 0500 LST. The OLR in this mode is basically contributed by the surface emission. To a first approximation, the diurnal variation of OLR shown in this mode is a clear manifestation of diurnal variation of surface temperature, which rises rapidly until afternoon and cools off slowly till the Sunrise of next day morning (Rosenberg et al., 1983). The diurnal cycle shown in the time variation of this mode is an indication that the three satellite configuration employed by the ERBE is good enough to adequately represent the diurnal variation of OLR. This mode explains 27.2% of the total normalized variance.

Presented in fig. 5a and 5b are the spatial pattern and the associated time variation of the EOF-3, respectively. In this pattern most of the variation occurs over cloudy regions. The time variation of this mode show a semi-diurnal cycle modulated by large amplitude diurnal cycle with maximum at 2000 LST and minimum at 0500 LST. Negative loadings are found over the deep convective cloudy regions, such as, the Congo river basin in southern part of Africa, maritime continent, Amazon and in a scattered way along the South Pacific Convergence Zone (SPCZ), South Atlantic Convergence Zone (SACZ) and the Inter Tropical Convergence Zone (ITCZ). The time variation of this mode indicate a peak in the evening, which means over these regions low OLR occurs in the evening. This OLR is emitted from the high level cold clouds present over these regions whose diurnal variation is consistent with the diurnal variation of OLR in this mode (Hartman and Recker,1986; Gruber and Chen, 1988; and Kondragunta and Gruber, 1994). Positive loadings in the spatial pattern are noticed mostly over the oceanic stratocumulus regions. Time variation indicates that minimum OLR occurs over these regions around 0500 LST. This is again in agreement with the low level cloudiness maximum over these regions which occurs around this time of the day (Hartman and Recker, 1986; Gruber and Chen, 1988; and Kondragunta and Gruber, 1994). So far, the diurnal part of variation in OLR is in excellent agreement with the earlier studies. However, the difficult part is accounting for the semi-diurnal variation most of which occurs in the negative side of time coefficients. Minnis et al. (1987) noticed semi-diurnal variation in cloudiness over the oceanic stratocumulus and trade cumulus regions. The phases of the semi-diurnal variation presented in this mode agree to some extent with those of Minnis et al. (1987) considering that they fitted a second harmonic to the data. They also suggested that the semi-diurnal pressure wave, forced by the atmospheric semi-diurnal tidal wave (Brier and Simpson, 1969), may be the likely cause for this variation. However, the discussion presented in the next section proved it to be otherwise. This mode explains 11.6% of the normalized variance.

4. Discussion

There are two possibilities that can cause the semi-diurnal variation noticed in the mode EOF-1. The first one is the differences in OLR retrieved from the instruments on board two different satellites. The second possibility is that the semi-diurnal variation is the true variation of the atmosphere and the possible cause is the atmospheric semi-diurnal tidal force. Strong evidence for the first possibility arises from a study by Minnis et al. (1991) who analyzed OLR from the NOAA-9, NOAA-10 and ERBS for the month of December, 1986. They found that over the oceanic regions, OLR fluxes retrieved from NOAA-9 and NOAA-10 are systematically lower and higher than the ones retrieved from the ERBS, respectively. In addition Gruber et al. (1994) and Ellingson et al. (1994) noticed that the daytime OLR fluxes from NOAA-9 are systematically lower than the nighttime ones. They also noticed that, in a zonal average sense, OLR fluxes from NOAA-9 are smaller than the ones from the ERBS during daytime. Furthermore, very convincing evidence was presented in a more detailed analysis performed by Thomas et al. (1994) where they investigated the biases in OLR retrievals from the ERBE scanners. They concluded that the daytime OLR retrievals from

NOAA-9 and NOAA-10 are biased and they are due to a longwave spectral correction. These biases are such that NOAA-9 under estimates and NOAA-10 over estimates with respect to the ERBS.

If one assumes that the OLR from the ERBS represents true fluxes at any instant, with the instrumental biases described before, the NOAA-9 fluxes will have lower than the true diurnal values around 0400 LST and 1500 LST and those from NOAA-10 will have higher than true diurnal values around 0800 LST and 2000 LST. Since the sampling is very high around the equator crossing times of the NOAA-9 and NOAA-10 compared to the ERBS, a semi- diurnal cycle with maxima at 0800 LST & 2000 LST and minima at 0400 LST and 1600 LST coinciding with the equator crossing times is expected in the OLR data. Also since Minnis et al. (1991) noticed the discrepancies over the oceanic cloudy regions, this kind of semi-diurnal cycle is expected mostly over the oceanic regions. The results presented in the first EOF mode are consistent with the above scenario. Therefore, we conclude that the semi-diurnal variation noticed in this mode is spurious. It is important to note that this type of semi-diurnal variation is predominant over the oceanic cloudy regions, especially over the stratocumulus regions, because the amplitude of the natural diurnal cycle itself is small over these regions. The possible reason for the large biases over the oceanic regions can be explained by referring to the OLR retrieval procedure in the ERBE algorithm. In the ERBE data processing algorithm, OLR is retrieved as a difference of total channel flux minus the shortwave channel during daytime and total channel flux itself during nighttime. If there is an error in retrieving reflected shortwave flux, that error will propagate into the longwave retrieval as well. This suggests that the biases in OLR come from the errors in retrieving reflected shortwave. This is confirmed by an independent analysis on the pixel scale by Thomas et al. (1994). Confirmation was also presented by the smaller instrumental biases in the relatively cloud free regions as shown in the EOF-2 mode which shows variation mostly over relatively cloud free continental regions. So the possible cause which could introduce biases in the OLR are consistent with the results presented in the first EOF mode. Moreover, a diurnal variation study of the International Satellite Cloud Climatology Project's (ISCCP) total cloudiness show a strong diurnal cycle as the dominant mode of variation in the first two EOF modes (Kondragunta and Gruber, 1994). Since OLR and cloudiness have inverse relationship, to a large extent in the tropical regions, the dominant modes of OLR also should show strong diurnal variation. If there were no instrumental biases in OLR, then the diurnal variation of OLR would have a minimum around 0500 LST and maximum around 2000 LST (Hartman and Recker, 1986; Gruber and Chen, 1988; and Kondragunta et al., 1993).

One might argue that the semi-diurnal variation shown in the EOF-1 is the true semi-diurnal mode of the atmospheric tidal oscillation. This possibility was checked by comparing our results with the existing literature on the semi-diurnal modes of the atmosphere (Chapman and Lindzen, 1970). The atmospheric semi-diurnal oscillations are caused by the atmospheric thermal tide. According to Brier and Simpson (1969), this tidal oscillation forces a semi-diurnal pressure wave in the tropics. These pressure fluctuations cause semi-diurnal variations in divergence and convergence fields, which in turn can cause fluctuations in cloudiness and

rainfall. The phases of these semi-diurnal variations in cloudiness occur at 0800 LST and 2000 LST (Brier and Simpson, 1969), which implies minimum OLR at these times. In the present study the phases of the semi-diurnal cycle shown in the EOF-1 mode do not agree with the phases of the diurnal cycle in the cloud field, supposedly forced by the atmospheric semi-diurnal tide. This rules out the possibility of the atmospheric semi-diurnal tidal wave as possible cause of the semi-diurnal oscillation noticed in the EOF-1 mode. This leaves us with the alternative that the retrieval bias is the main candidate responsible for the semi-diurnal variation noticed in the mode EOF-1.

To demonstrate that the semi-diurnal variation noticed in the first EOF mode is not an artifact of the analysis procedure employed in this study, composite diurnal variation of OLR at a few selected grid points were examined. Presented in figure 6a is the time series of composite OLR at a grid point over the stratocumulus cloudy region in the S.E. Atlantic. A semi-diurnal cycle whose maxima and minima coinciding with equator crossing times of the NOAA-9 and NOAA-10 is obvious in this curve. Both cubic spline and linear interpolation techniques clearly show similar variation. The difference between the maximum and minimum is about 9 Wm^{-2}. From the regression relationships given by Minnis et al., (1991) (for the month of December 1986, during daytime over oceanic regions: NOAA9 = -4.77 + 0.99*ERBS and NOAA10 = 3.93 + 0.99*ERBS), for a given value of 270 Wm^{-2} from the ERBS, the bias in NOAA-9 is 7.5 Wm^{-2} lower and NOAA-10 is 1.2 Wm^{-2} higher, with respect to the ERBS. The net difference is 8.7 Wm^{-2} which is in close agreement with the amplitude of semi-diurnal cycle noticed in this time series. Since biases in the NOAA-9 and NOAA-10 are in opposite directions with respect to the ERBS, they add up and show up as a semi-diurnal cycle in the analysis presented in this study. Gruber et al. (1994) also noticed similar differences of the order of about 4 Wm^{-2} between NOAA-9 and ERBS (NOAA < ERBS) during daytime in zonal averages for the month of April 1985. Minnis et al. (1991) also reported that the differences in OLR fluxes between NOAA-9 and ERBS during daytime have almost doubled since the beginning of the experiment to demise of the NOAA-9 scanner.

Another such time series is presented in figure 6b which shows the variation of composite OLR at a grid point over the S.E. Pacific. This also clearly shows the effect described above. A grid point over the Andes (fig. 6c) was chosen to demonstrate that such instrumental bias is minimum over relatively cloud free regions. The time series at this grid point show the true diurnal variation of OLR remarkably well. Excellent agreement of this with the results of Harrison et al (1988) based on GOES data confirms the validity of the analysis presented in this study. It is interesting to note that the OLR peak in this time series occurs near noon, unlike over the Sahara (fig. 2) where the peak occurs in the afternoon. This suggests that over elevated places OLR peak occurs near noon. Of course, it should be noted that the phase of the OLR over dry continental regions depends on the soil type and soil moisture content, in addition to the elevation. In summary, instrumental biases are noticed only over cloudy regions as depicted by EOF-1 and EOF-3 modes (also figures 6a and 6b) and virtually absent over relatively cloud free regions as depicted by EOF-2 (also figs. 2 and 6c).

What makes this study more interesting is the effect of the instrumental bias, as presented in this study, on the global averages of OLR. Figure 7 shows the time series of monthly mean global averages of OLR from the NOAA-9 and ERBS combined (February 1985 to January 1987), and NOAA-10 and ERBS combined (December 1986 to May 1989) period. Note that December 1986 and January 1987 have data from all three satellites. The dominant oscillation of this time series is the annual cycle . In addition, there is a sudden jump in the time series from the period NOAA-9 and ERBS combined to NOAA-10 and ERBS combined. This sudden jump in the time series is consistent with the biases in the OLR retrieval from the different instruments discussed in this paper. Kyle et al. (1993) showed that global (60°N to 60°S) longwave mean of NOAA-9 is smaller by 5.2 Wm^{-2} and of NOAA-10 is larger by 3.1 Wm^{-2} with respect to the ERBS for December 1986. Though they attributed these differences to different diurnal sampling times, they did not rule out the possibility of diurnal averaging methods and calibration differences. This study mainly points to the biases present in the OLR data and not aimed at making any corrections. Nevertheless, the biases in the OLR data, as presented in this study, have significant contribution to the biases in the global means as shown in figure 7. In order to maximize utilization of the ERBE OLR data for climate change detection or model validation, it is necessary that these biases be corrected. Since there are no ground truth measurements for the top of the atmosphere radiation budget parameters, one way to adjust these biases is to consider the OLR from the ERBS as standard. This enables the OLR data to be uniform throughout the experiment period. Additionally, one may consider using alternative methods for obtaining OLR when reprocessing the data.

5. Concluding Remarks

The OLR data from the ERBE three satellite combination were analyzed to study the duirnal variation. The first EOF mode which explains the largest normalized variance indicates a strong semi-diurnal signal. It was argued that this semi-diurnal signal is not realistic and is caused by the systematic biases in the retrieval of the OLR from different instruments on board different satellites, viz., NOAA-9 and NOAA-10. This conclusion was drawn based on the facts that (i) the phases of the semi-diurnal variation noticed in the first EOF mode agree with the equator crossing times of the NOAA-9 and NOAA-10 satellites, (ii) There was ample evidence for systematic biases in OLR retrieval from earlier studies and (iii) the semi-diurnal cycle shown in the first EOF mode is not supported by the atmospheric tidal theory as a possible mechanism. A true and strong diurnal signal over the relatively cloud free continental regions, as shown by the second EOF mode, presents strengths to the analysis procedure employed in this study. This also confirms that the three satellite orbital configuration employed by the ERBE gives reasonable diurnal sampling of OLR approximately over a period of a month. This study calls for reprocessing of the OLR from the ERBE scanner instruments with the biases corrected. A reprocessed OLR data set during the period when all three ERBE satellites were operating will be useful to obtain diurnal variation without resorting to any artificial modeling and hence invaluable for climate model validation purposes.

Acknowledgements

The authors would like to thank one of the anonymous reviewers whose comments on an earlier version of the paper was key to the evolution of this paper. Thanks also to Drs. Dan Tarpley and Herbert Jacobowitz of ORA/NESIDS/NOAA for useful comments, and to Dr. Lee Kyle of NASA/Goddard Space Flight Center for providing global averages of OLR and for useful discussions on several occasions.

References

Barkstrom, B. R., 1984: The Earth Radiation Budget Experiment (ERBE). *Bull. Am. Meteor. Soc.*, 65, 1170-1185.

-------, G. Harrison, R. Green, J. Kibler, R. D. Cess, and the ERBE Science Team, 1989: Earth Radiation Budget Experiment (ERBE) archival and April 1985 results. *Bull. Am. Meteorol. Soc.*, 70, 1254-1262.

Brier, G. W. and J. Simpson, 1969: Tropical cloudiness and rainfall related to pressure and tidal variations. *Quart. J. Roy.Meteorol. Soc.*, 95,120-147.

Brooks, D. R., E. F. Harrison, P. Minnis, J. T. Sutteles and R. S. Kandel, 1986: Development of algorithms for understanding the temporal and spatial variability of the earth's radiation balance. *Rev. of Geophys.*, 24, 422-438.

-------, and P. Minnis, 1984: Comparison of longwave diurnal models applied to simulation of the Earth Radiation Budget Experiment. *J. Clim. Appl. Meteorol.*, 23, 155-160.

Chapman, S. and R. S.Lindzen, 1970: Atmospheric Tides, Thermal and Gravitational. Gordon and Breach/Science Publishers, New York, 200 p.

Chelliah, M. and P. Arkin, 1992: Large-scale interannual variability of monthly outgoing longwave radiation anomalies over the global tropics. *J. Climate*, 5, 371-389.

Cheruy, F., R. S. Kandel, and J. P. Duvel, 1991: Outgoing Longwave Radiation and its diurnal variation from combined Earth Radiation Budget Experiment and Meteosat observations. 2. Using Meteosat data to determine the longwave diurnal cycle. *J. Geophys. Res.*, 96, 22,623 - 22,630.

Ellingson, R. G., H. T. Lee, D. Yanuk and A. Gruber, 1994: Validation of a technique for estimating outgoing longwave radiation from HIRS radiance observations. J. Atmos. Oceanic. Technol., 11, 357-365.

Gruber, A, P. Ardanuy, M. Weiss, S.K. Yang, R.G. Ellingson and S.N. Oh, 1994: A comparison of ERBE and AVHRR longwave flux estimates. *Bull. Am. Meteorol. Soc.*, In press.

-------, and T. S. Chen, 1988: Diurnal variation of outgoing longwave radiation, *J. Climatology,* 8, 1-16.

Harrison, E. F., D. R. Brooks, P. Minnis, B. A. Wielicki, W. F. Staylor, G. G. Gibson, D. E. Young, F. M. Denn and the ERBE science team, 1988: First estimates of the diurnal variation of longwave radiation from the multiple satellite Earth Radiation Budget Experiment (ERBE). *Bull. Amer. Meteor. Soc.*, 69, 10, 1144-1151.

Hartman, D. L. and E. E. Recker, 1986: Diurnal variation of outgoing longwave radiation in tropics. *J. Clim. Appl. Meteor.*, 25, 800-812.

Kidson, J. W., 1975: Eigenvector analysis of monthly mean surface data. *Mon. Wea. Rev.*, 103, 177-186.

Kondragunta, C. R. and Gruber,1994: Diurnal variation of the ISCCP cloudiness. *Geophy. Res. Letters*, 21, 2015-2018.

--------, H. L. Kyle and A. T. Micherikunnel, 1993: Diurnal variation of the Outgoing Longwave Radiation as revealed by the E. R. B. E., *Tellus*, 45A, 1-14.

Kutzbach, J. E., 1967: Empirical Eigenvectors of sea level pressure, surface temperature and precipitation complexes over North America. *J. Appl. Meteor.*, 6, 791-802.

Kyle, H. L., J.R. Hickey, P. E. Ardanuy, H. Jacobowitz, A. Arking, G. G. Campbell, F. B. House, R. Maschhoff, G. L. Smith, L. L. Stowe and T. Vonder Haar, 1993: The Nimbus Earth Radiation Budget Experiment: 1975 to 1992. *Bull. Am. Meteor. Soc.*, 74, 815-830.

Meisner, B. N. and P. A. Arkin, 1987: Spatial and annual variation in the diurnal cycle of large scale tropical convective cloudiness and precipitaion. *Mon. Wea. Rev.*, 115, 2009-2032.

Minnis, P., E. Harrison, D. Doelling, A. Fan, D. Young and G. Gibson, 1991: Examination of NOAA-9, NOAA-10 and ERBS scanner intercalibration with TSA results. 28th ERBE Science Team Meeting, March 26-27.

-------, and -------, 1984a: Diurnal variability of regional cloud and clear-sky radiative parameters derived from GOES data Part II: November 1978 cloud distributions. *J. Clim. Appl. Meteorol.* 23, 1012-1031.

-------, and -------, 1987: Cloud cover over the equatorial eastern Pacific derived from July 1983 International Satellite Cloud Climatology Project data using a hybrid bispectral threshold method. *J. Geophys. Res.*, 92, 4051-4073.

Riehl, H., 1979: Climate and Weather in the tropics, Academic press, pp 611.

Rosenburg, N. T., B. L. Blad, and S. B. Verma, 1983: Microclimate. Published by John Wiley & sons. pp 495.

Smith, G. L., D. Rutan, T. P. Charlock, and T. D. Bess, 1990: Annual and interannual variations of absorbed solar radiation based on a 10-year data set. *J. Geophys. Res.*, 95, 16,639-16,652.

Thomas, D., J. P. Duvel and R. Kandel, 1994: Diurnal bias in calibration of broad-band radiance measurements from space. In press, IEEE TGARS.

List of Tables

Table 1. Latitude versus local solar time OLR sampling at longitude 1.25°E. The number in each column indicates the number of times that particular local hour was sampled by one of the three ERBE satellites during the entire study period. Data are shown at alternate latitude bands.

List of Figures

Figure 1. Time series of the hourly OLR obtained from the cubic spline interpolation (solid) and linear interpolation (dotted) over the Sahara desert at 1.25°E, 23.75°N. Only a segment of the time series is shown.

Figure 2. Composite diurnal variation of the average sky OLR obtained from cubic spline interpolation (solid) and monthly hourly OLR obtained from the ERBE data processing scheme (dotted) over the Sahara desert at 1.25°E, 23.75°N.

Figure 3. (a) Spatial mode of the EOF-1 expressed in terms of correlation coefficient and (b) time variation of the EOF-1 mode

Figure 4. Same as in figure 3, except for the mode EOF-2

Figure 5. Same as in figure 3, except for the mode EOF-3

Figure 6. Time series of the composite OLR for grid points (a) S.E. Atlantic, (b) S.E. Pacific and (c) Andes. Time series with open and closed circles are obtained from the cubic spline and linear interpolation, respectively.

Figure 7. Time series of the global average OLR from the ERBE

Table 1. Latitude versus local solar time OLR sampling at longitude 1.25°E. The number in each column indicates the number of times that particular local hour was sampled by one of the three ERBE satellites during the entire study period. Data are shown at alternate latitude bands.

	LOCAL SOLAR TIME																							
LAT.	1	2	3	4	5	6	7	8	9	10	11	12	13	14	15	16	17	18	19	20	21	22	23	24
88.75	32	35	34	32	34	34	36	34	35	34	34	36	34	37	34	34	35	34	36	32	34	32	31	36
83.75	19	22	17	20	25	28	32	32	38	36	36	39	36	39	33	34	38	34	26	17	17	2	0	5
78.75	0	13	20	26	26	26	31	33	38	36	37	39	36	39	36	34	33	27	25	20	6	0	0	0
73.75	0	2	21	29	25	27	29	35	38	36	37	42	37	39	37	37	29	26	26	23	5	0	0	0
68.75	0	0	20	28	26	27	27	35	38	37	37	42	30	25	29	34	28	27	23	27	2	0	0	1
63.75	8	9	22	30	33	31	30	28	29	30	14	27	28	27	26	22	21	26	25	27	1	3	5	7
58.75	10	10	23	29	33	34	17	26	32	27	12	11	29	29	29	20	4	25	26	25	2	5	6	7
53.75	11	11	24	29	32	31	14	30	33	20	14	10	25	29	29	19	1	19	24	25	3	6	7	9
48.75	11	13	23	31	35	22	16	29	35	18	13	11	16	30	29	20	2	10	25	26	3	7	8	9
43.75	8	8	22	30	32	14	14	24	36	9	10	7	5	26	30	21	1	5	25	26	4	7	7	6
38.75	6	6	22	29	25	9	11	30	25	8	8	5	3	21	28	23	3	3	25	28	5	4	5	5
33.75	5	4	19	31	22	9	9	32	26	6	6	5	4	17	28	22	3	3	22	28	6	5	5	4
28.75	5	5	20	30	19	7	8	32	25	4	4	4	4	14	30	23	4	4	20	28	6	4	4	4
23.75	4	4	19	29	16	8	7	31	25	3	4	4	4	13	28	24	3	5	16	29	6	5	4	3
18.75	4	4	20	29	11	7	7	32	20	4	4	4	4	9	28	21	3	5	13	30	6	3	4	3
13.75	3	4	20	27	8	6	10	31	19	4	3	3	4	8	28	24	3	5	14	30	9	2	4	4
8.75	2	3	24	28	9	6	13	29	16	4	4	3	4	4	27	23	3	5	14	29	9	3	4	4
3.75	3	4	26	28	4	5	12	30	10	4	3	3	4	4	28	24	4	5	15	28	11	3	3	3
-1.25	3	4	27	26	4	7	13	30	8	4	4	3	3	4	26	28	4	7	14	28	10	3	3	4
-6.25	3	3	28	27	3	5	16	30	8	3	4	3	4	3	26	28	4	5	12	28	12	4	3	4
-11.25	4	5	28	26	2	3	19	27	8	4	3	3	4	3	25	28	6	8	9	29	13	3	3	4
-16.25	3	8	27	26	3	3	19	27	6	4	3	4	4	2	23	29	9	9	7	29	16	4	4	4
-21.25	4	10	28	23	3	5	18	27	6	4	3	4	4	3	24	29	13	7	9	30	18	4	3	4
-26.25	5	12	28	22	4	4	20	27	8	5	3	4	4	4	25	31	17	7	9	29	21	4	3	5
-31.25	4	13	28	21	4	5	24	28	5	4	5	5	5	4	25	30	19	8	8	29	24	6	4	4
-36.25	5	17	30	19	3	3	25	29	5	5	4	5	5	5	25	30	23	9	9	29	29	7	4	5
-41.25	5	22	29	21	2	6	26	29	5	6	6	7	7	6	24	33	30	11	16	26	29	13	9	6
-46.25	9	27	29	22	2	9	27	29	4	7	7	10	12	13	33	36	33	19	16	30	31	20	10	8
-51.25	17	27	29	22	1	16	26	29	3	5	7	10	12	12	31	36	33	20	15	31	31	25	13	10
-56.25	28	26	27	22	0	25	26	30	2	4	6	9	11	11	30	35	33	24	14	31	30	30	12	10
-61.25	31	24	28	20	12	28	26	28	1	3	5	7	10	9	30	33	31	27	22	31	32	27	20	23
-66.25	26	26	28	31	27	27	27	26	1	1	2	5	7	6	28	30	28	27	31	40	27	29	41	35
-71.25	29	26	30	23	24	28	26	26	3	0	0	0	0	1	24	25	28	26	26	29	27	28	34	29
-76.25	40	34	37	36	27	27	26	25	5	0	0	0	0	9	22	26	27	26	27	37	35	37	38	35
-81.25	38	35	37	38	35	33	26	21	10	0	0	0	4	20	20	24	26	27	29	33	35	35	39	36
-86.25	38	35	30	31	33	38	32	30	24	29	19	24	20	22	19	18	29	39	33	32	34	37	39	34

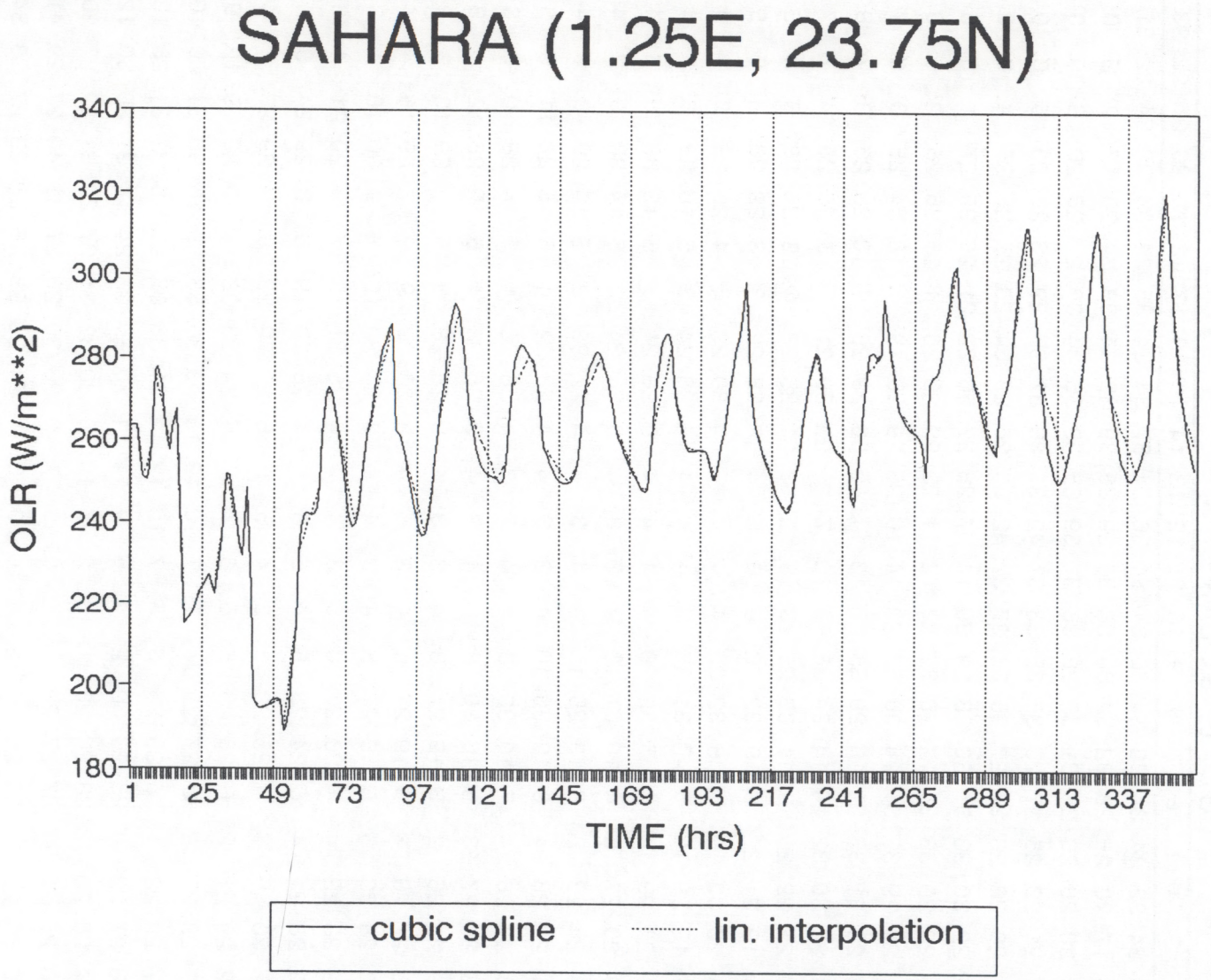

Figure 1. Time series of the hourly OLR obtained from the cubic spline interpolation (solid) and linear interpolation (dotted) over the Sahara desert at 1.25°E, 23.75°N. Only a segment of the time series is shown.

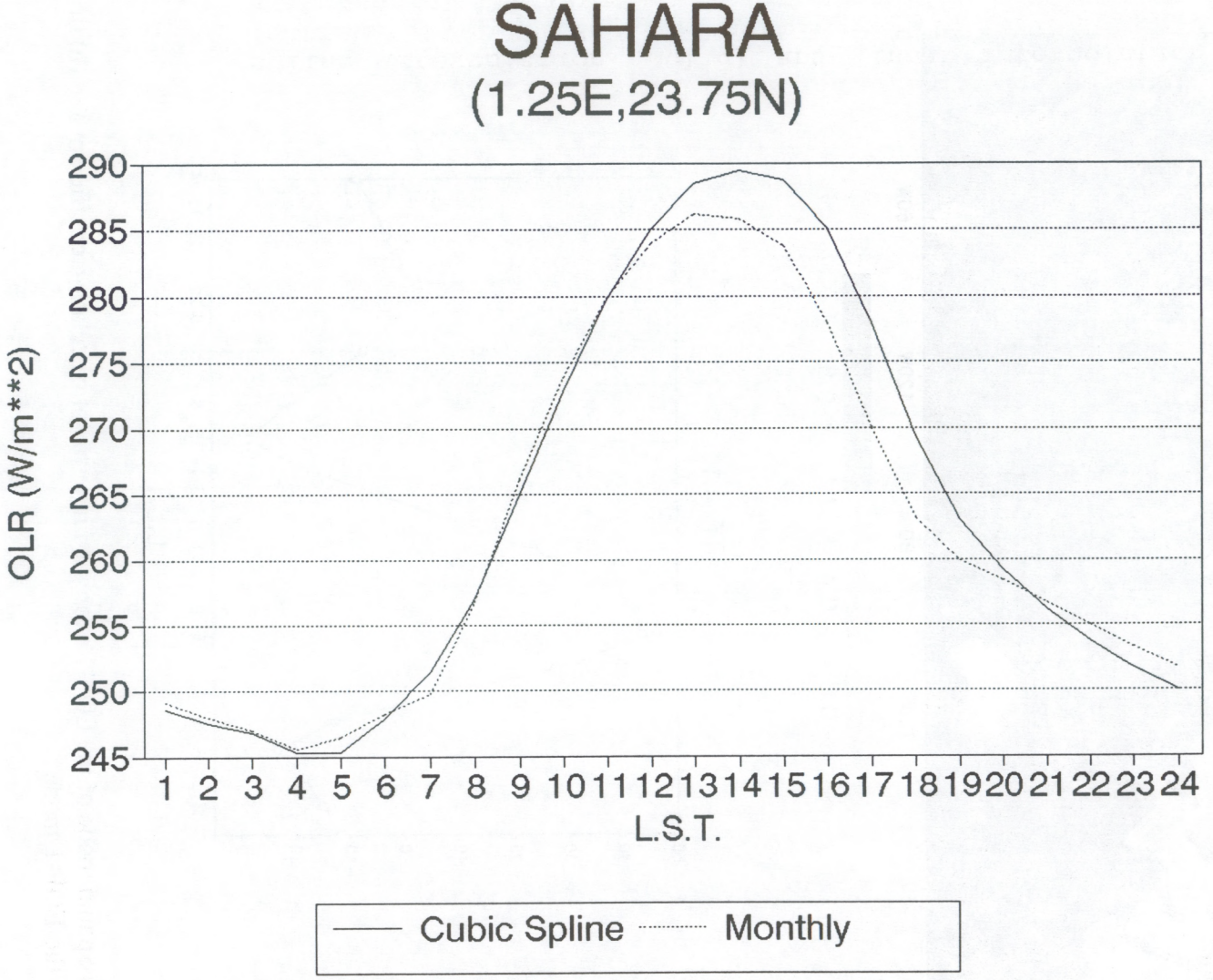

Figure 2. Composite diurnal variation of the average sky OLR obtained from cubic spline interpolation (solid) and monthly hourly OLR obtained from the ERBE data processing scheme (dotted) over the Sahara desert at 1.25°E, 23.75°N.

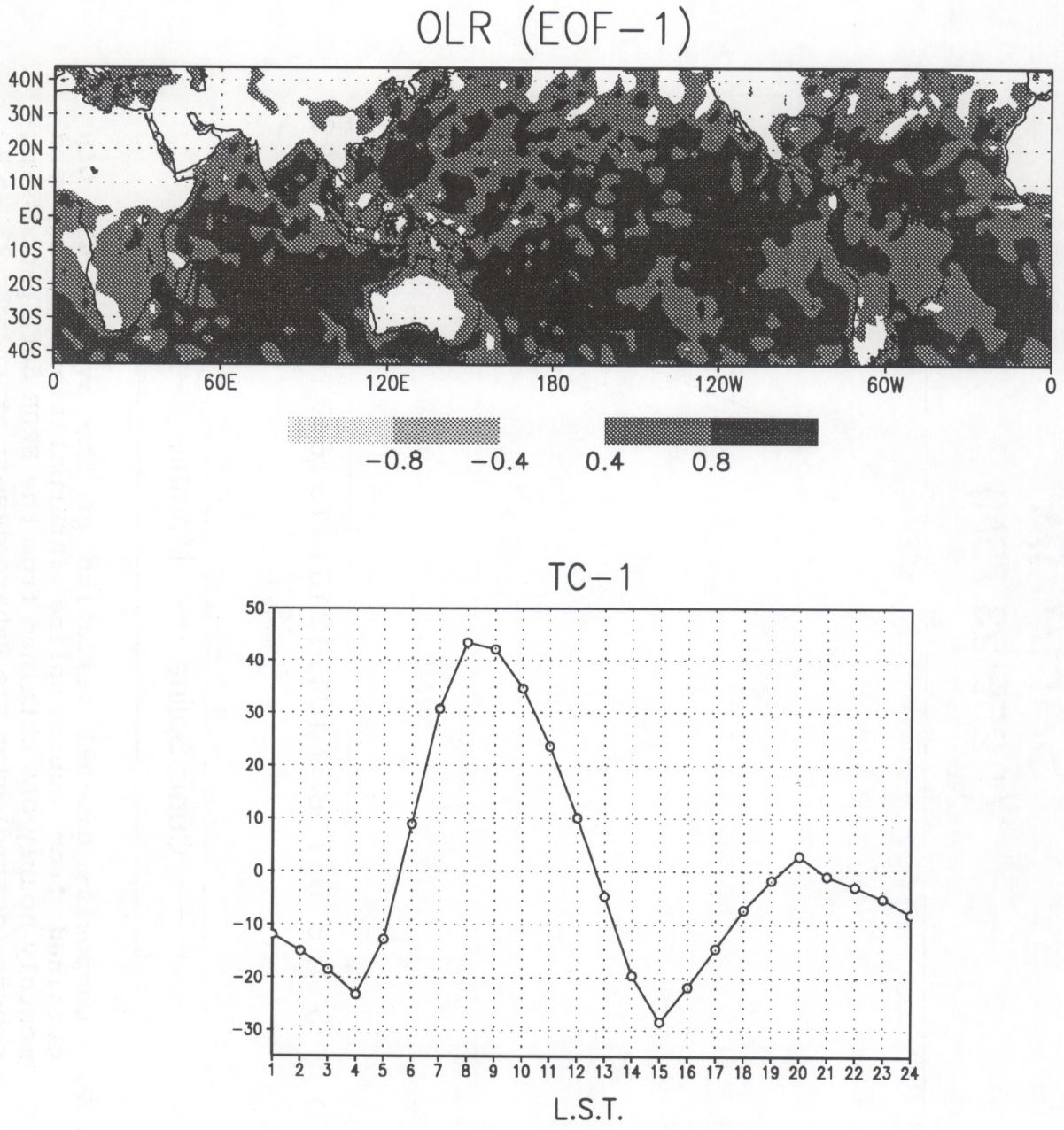

Figure 3. (a) Spatial mode of the EOF-1 expressed in terms of correlation coefficient and (b) time variation of the EOF-1 mode

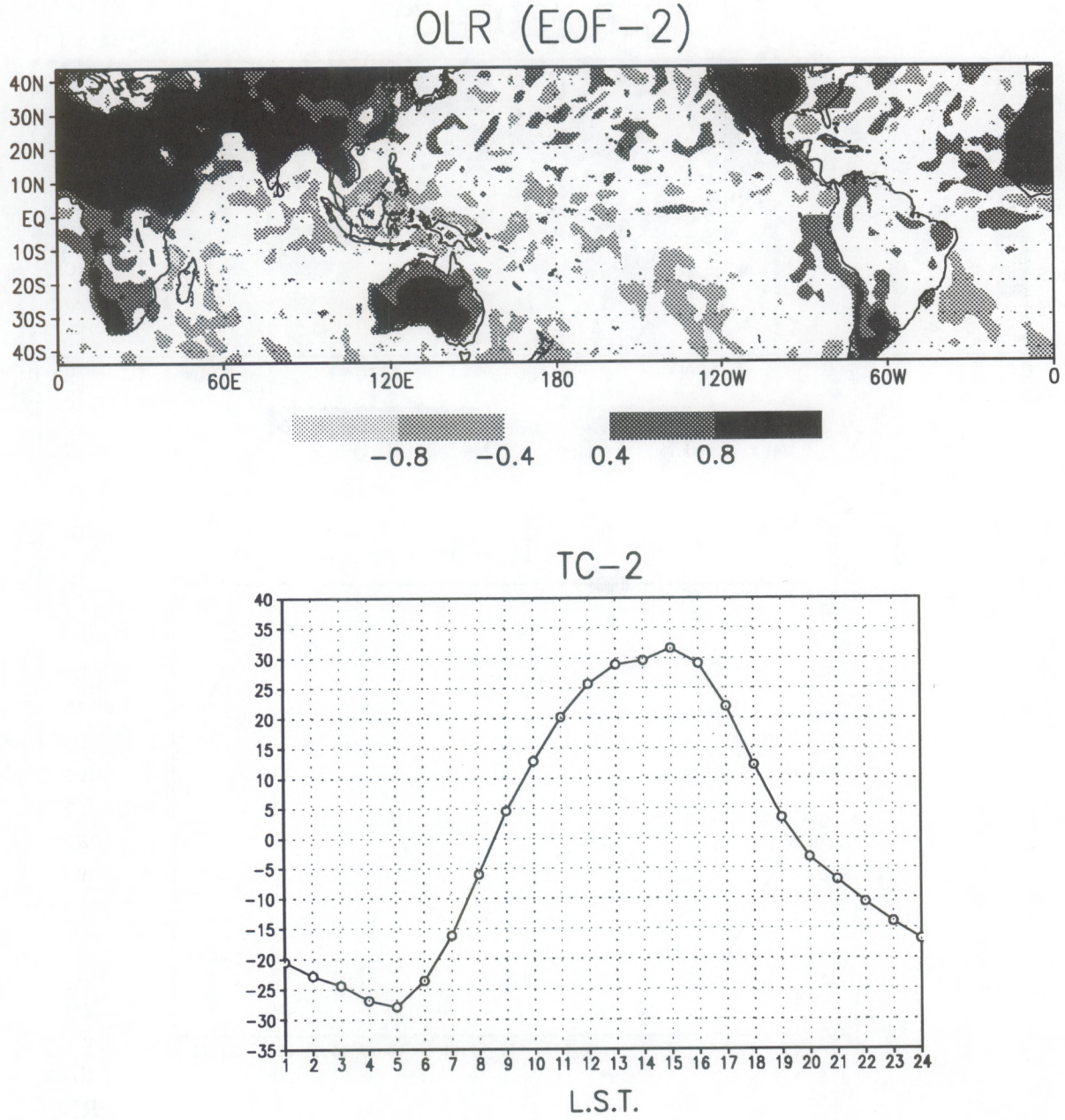

Figure 4. Same as in figure 3, except for the mode EOF-2

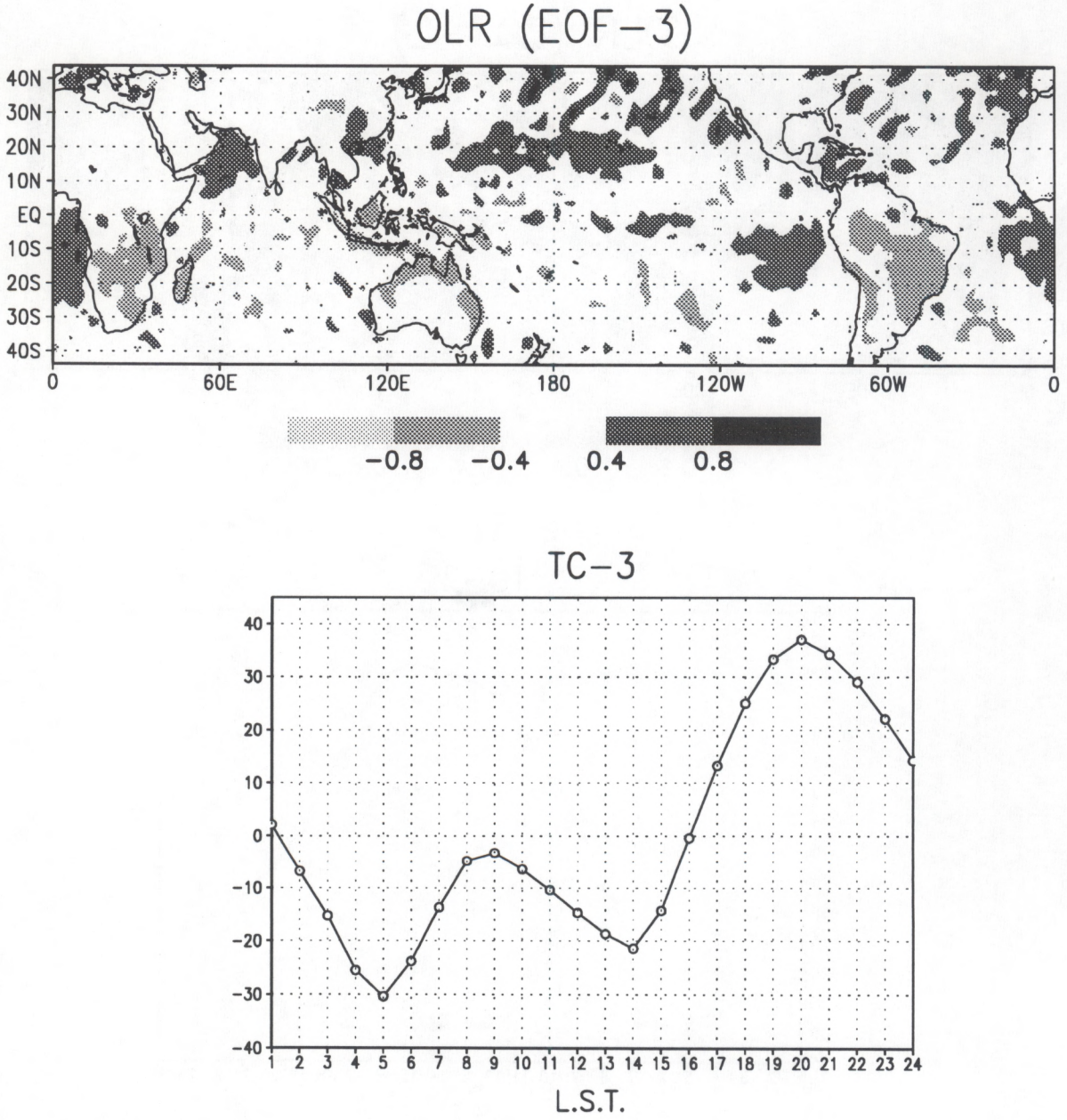

Figure 5. Same as in figure 3, except for the mode EOF-3

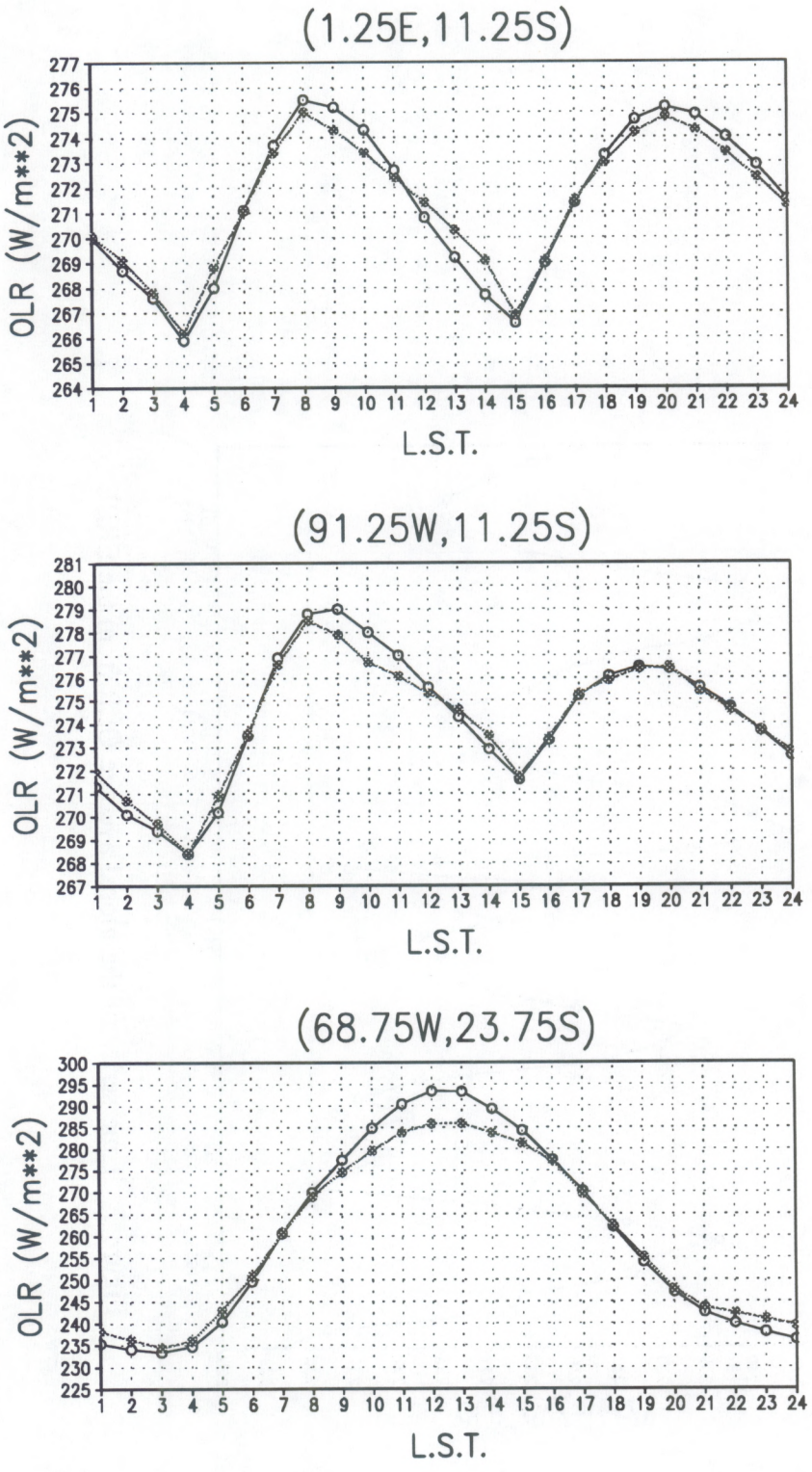

Figure 6. Time series of the composite OLR for grid points (a) S.E. Atlantic, (b) S.E. Pacific and Andes. Time series with open and closed cicles are obtained from the cubic spline and linear interpolation, respectively.

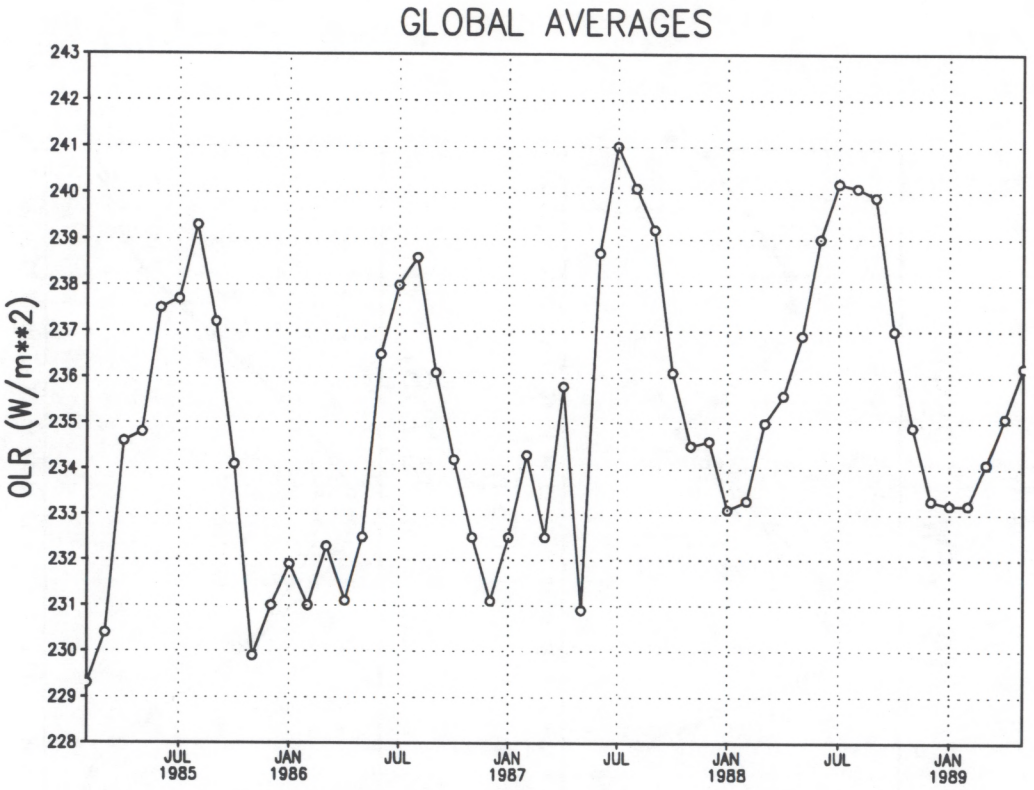

Figure 7. Time series of the global average OLR from the ERBE

(Cont'd from front inside cover)

NESDIS 49 Implementation of Reflectance Models in Operational AVHRR Radiation Budget Processing. V. Ray Taylor, February 1990.

NESDIS 50 A Comparison of ERBE and AVHRR Longwave Flux Estimates. A. Gruber, R. Ellingson, P. Ardanuy, M. Weiss, S. K. Yang, (Contributor: S.N. Oh).

NESDIS 51 The Impact of NOAA Satellite Soundings on the Numerical Analysis and Forecast System of the People's Republic of China. A. Gruber and W. Zonghao, May 1990.

NESDIS 52 Baseline Upper Air Network (BUAN) Final Report. A. L. Reale, H. E. Fleming, D. Q. Wark, C. S. Novak, F. S. Zbar, J. R. Neilon, M. E. Gelman and H. J. Bloom, October 1990.

NESDIS 53 NOAA-9 Solar Backscatter Ultraviolet (SBUV/2) Instrument and Derived Ozone Data: A Status Report Based on a Review on January 29, 1990. Walter G. Planet, June 1990.

NESDIS 54 Evaluation of Data Reduction and Compositing of the NOAA Global Vegetation Index Product: A Case Study. K. P. Gallo and J. F. Brown, July 1990.

NESDIS 55 Report of the Workshop on Radiometric Calibration of Satellite Sensors of Reflected Solar Radiation, March 27-28, 1990, Camp Springs, MD. Peter Abel (Editor), July 1990.

NESDIS 56 A Noise Level Analysis of Special 10-Spin-Per-Channel VAS Data. Donald W. Hillger, James F. W. Purdom and Debra A. Lubich, February 1991.

NESDIS 57 Water Vapor Imagery Interpretation and Applictions to Weather Analyis and Forecasting. Roger B. Weldon and Susan J. Holmes, April 1991.

NESDIS 58 Evaluating the Design of Satellite Scanning Radiometers for Earth Radiation Budget Measurements with System, Simulations. Part 1: Instantaneous Estimates. Larry Stowe, Philip Ardanuy, Richard Hucek, Peter Abel and Herbert Jacobowitz, October 1991.

NESDIS 59 Interactive Digital Image Display and Analysis System (IDIDAS) User's Guide. Peter J. Celone and William Y. Tseng, October 1991.

NESDIS 60 International Dobson Data Workshop Summary Report. Robert D. Hudson (University of Maryland) and Walter G. Planet, February 1992.

NESDIS 61 Tropical Cyclogenesis in the Western North Pacific. Raymond M. Zehr, July 1992.

NESDIS 62 NOAA Workshop on Climate Scale Operational Precipitation and Water Vapor Products. Ralph Ferraro (Editor), October 1992.

NESDIS 63 A Systematic Satellite Approach for Estimating Central Pressures of Mid-Latitude Oceanic Storms. Frank J. Smigielski and H. Michael Mogil, December 1992.

NESDIS 64 Adjustment of TIROS Operational Vertical Sounder Data to a Vertical View. David Q. Wark, March 1993.

NESDIS 65 A Noise Level Analysis of Special Multiple-Spin VAS Data During Storm-fest. Donald W. Hillger, James F.W. Purdom and Debra A. Molenar, April 1993.

NESDIS 66 Catalogue of Heavy Rainfall Cases of Six Inches or more over the Continental U.S. during 1992. Charles Kadin, April 1993.

NESDIS 67 The Relationship between Water Vapor Plumes and Extreme Rainfall Events during the Summer Season. Wassila Thiao, Roderick A. Scofield and Jacob Robinson, May 1993.

NESDIS 68 AMSU-A Engineering Model Calibration. Tsan Mo, Michael P. Weinreb, Norman C. Grody and David Q. Wark, June 1993.

NESDIS 69 Nonlinearity Corrections for the Thermal Infrared Channels of the Advanced Very High Resolution Radiometer: Assessment and Recommendations. C.R. Nagaraja Rao (Editor), June 1993.

NESDIS 70 Degradation of the Visible and Near-Infrared Channels of the Advanced Very High Resolution Radiometer on the NOAA-9 Spacecraft: Assessment and Recommendations for Corrections. C.R. Nagaraja Rao (Editor), June 1993.

NESDIS 71 Spectral Radiance-Temperature Conversions for Measurements by AVHRR Thermal Channels 3,4,5. Paul A. Davis, August 1993.

NESDIS 72 Summary of the NOAA/NESDIS Workshop on Development of a Global Satellite/in Situ Environmental Database. Edited by K.P. Gallo and D.A. Hastings, August 1993.

NESDIS 73 Intercomparison of the Operational Calibration of GOES-7 and METEOSAT-3/4. W. Paul Menzel, Johannes Schmetz, Steve Nieman, Leo Van de Berg, Volker Gaertner, and Timothy J. Schmit, September 1993.

NESDIS 74 Dobson Data Re-Evaluation Handbook. Robert D. Hudson and Walter G. Planet (Eds), October 1993.

NESDIS 75 Detection and Analysis of Fog at Night Using GOES Multispectral. Gary P. Ellrod, February 1994.

NESDIS 76 Tovs Operationa Sounding Updgrades: 1990-1992. A. Reale, M. Chalfant, R. Wagoner, T. Gardner and L. Casey, March 1994.

NESDIS 77 NOAA Polar Satellite Calibration: A System Description. Cecil A. Paris, April 1994.

NESDIS 78 Post-Launch Calibration of the Visible and Near Infrared Channels of the Advanced Very High Resolution Radiometer on NOAA-7,-9, and -11 Spacecraft. C. R. Nagaraja Rao and Jianhua Chen, April 1994.

NESDIS 79 Quality Control and Processing of Historical Oceanographic Nutrient Data. Margarita E. Conkright, Timothy P. Boyer and Sydney Levitus, April 1994.

NOAA SCIENTIFIC AND TECHNICAL PUBLICATIONS

The National Oceanic and Atmospheric Administration was established as part of the Department of Commerce on October 3, 1970. The mission responsibilities of NOAA are to assess the socioeconomic impact of natural and technological changes in the environment and to monitor and predict the state of the solid Earth, the oceans and their living resources, the atmosphere, and the space environment of the Earth.

The major components of NOAA regularly produce various types of scientific and technical information in the following kinds of publications:

PROFESSIONAL PAPERS - Important definitive research results, major techniques, and special investigations.

CONTRACT AND GRANT REPORTS - Reports prepared by contractors or grantees under NOAA sponsorship.

ATLAS - Presentation of analyzed data generally in the form of maps showing distribution of rainfall, chemical and physical conditions of oceans and atmosphere, distribution of fishes and marine mammals, ionospheric conditions, etc.

TECHNICAL SERVICE PUBLICATIONS - Reports containing data, observations, instructions, etc. A partial listing includes data serials; prediction and outlook periodicals; technical manuals, training papers, planning reports, and information serials; and miscellaneous technical publications.

TECHNICAL REPORTS - Journal quality with extensive details, mathematical developments, or data listings.

TECHNICAL MEMORANDUMS - Reports of preliminary, partial, or negative research or technology results, interim instructions, and the like.

U.S. DEPARTMENT OF COMMERCE
National Oceanic and Atmospheric Administration
National Environmental Satellite, Data, and Information Service
Washington, D.C. 20233